Am. J. Hum. Genet. 48:687–695, 1991

A Human Gene Homologous to the Formin Gene Residing at the Murine Limb Deformity Locus: Chromosomal Location and RFLPs

Richard L. Maas,*'§ Lisa I. Jepeal,§ Sandra L. Elfering,§ Randall F. Holcombe,‖ Cynthia C. Morton,† Roger L. Eddy,# Mary G. Byers,# Thomas B. Shows,# and Philip Leder‡'§

Departments of *Medicine, †Pathology, and ‡Genetics and §Howard Hughes Medical Institute, Brigham and Women's Hospital and Harvard Medical School, Boston; ‖Section of Hematology-Oncology, Louisiana State University Medical Center, Shreveport; and #Roswell Park Memorial Institute, Buffalo

Summary

The murine limb deformity (*ld*) locus resides on mouse chromosome 2 and gives rise to a recessively inherited, characteristic limb deformity/renal aplasia phenotype. In this locus in the mouse, a gene, termed the "formin" gene, has been identified which encodes an array of differentially processed transcripts in both adult and embryonic tissues. A set of these transcripts are disrupted in independent mutant mouse *ld* alleles. We wish to report the isolation of a human genomic clone which is homologous to the mouse formin gene by virtue of sequence comparison and expression of conserved exons. Among human fetal tissues analyzed, the kidney appears to be a major site of expression. This human gene, *LD,* maps to chromosome 15q11→qter in mouse human somatic cell hybrids and, specifically, to 15q13→q14 by chromosomal in situ hybridization. This localization establishes both *LD* and β_2-microglobulin as syntenic genes on mouse chromosome 2 and human chromosome 15 and implies the interspecies conservation of the region between them. In addition, we identify in the human locus two frequently occurring DNA polymorphisms which can be used to test the linkage of *LD* to known human dysmorphoses.

Introduction

The murine limb deformity (*ld*) locus is a genetic region defined by several different noncomplementing mutant alleles which share a characteristic limb deformity and variably penetrant renal aplasia phenotype (Woychik et al. 1985, 1990*a;* Green 1981; Messing et al. 1990). The limb deformity is marked by synostoses and syndactyly of all four limbs. The renal defect is marked by unilateral or bilateral renal aplasia (Kleinebrecht et al. 1982; R. L. Maas, unpublished data). During the course of studies on transgene-induced tumorigenesis, a fortuitous transgenic insertion resulted in the formation of a mutant *ld* allele, termed "ld^{Hd}" (Woychik et al. 1985). To test the hypothesis that the transgene had disrupted an endogenous gene, adjacent mouse flanking sequences were cloned and used to detect RFLPs segregating with the mutant phenotype in the transgenic and two spontaneous alleles, ld^{J} and ld^{OR}. Several regions close to the transgene insertion were tentatively identified as exons by virtue of both similarity to human sequences and the presence of open reading frames between consensus splice donor and acceptor sequences.

Using a sensitive RNAse protection assay and several of the conserved sequences as probes, we have identified in the mouse a complex gene which, because of its presumed role in the formation of limbs and kidneys, has been assigned the name "formin" gene (Woychik et al. 1990*b*). The likely involvement of this gene product in the limb deformity phenotype stems from the following observations: it is the only discrete transcription unit thus far identified at the transgene insertion site; its expression in early development oc-

Received September 18, 1990; revision received November 20, 1990.

Address for correspondence and reprints: Richard Maas, M.D., Ph.D., Department of Medicine, Brigham and Women's Hospital, 75 Francis Street, Boston, MA 02115.

0002-9297/91/4804-0007$02.00

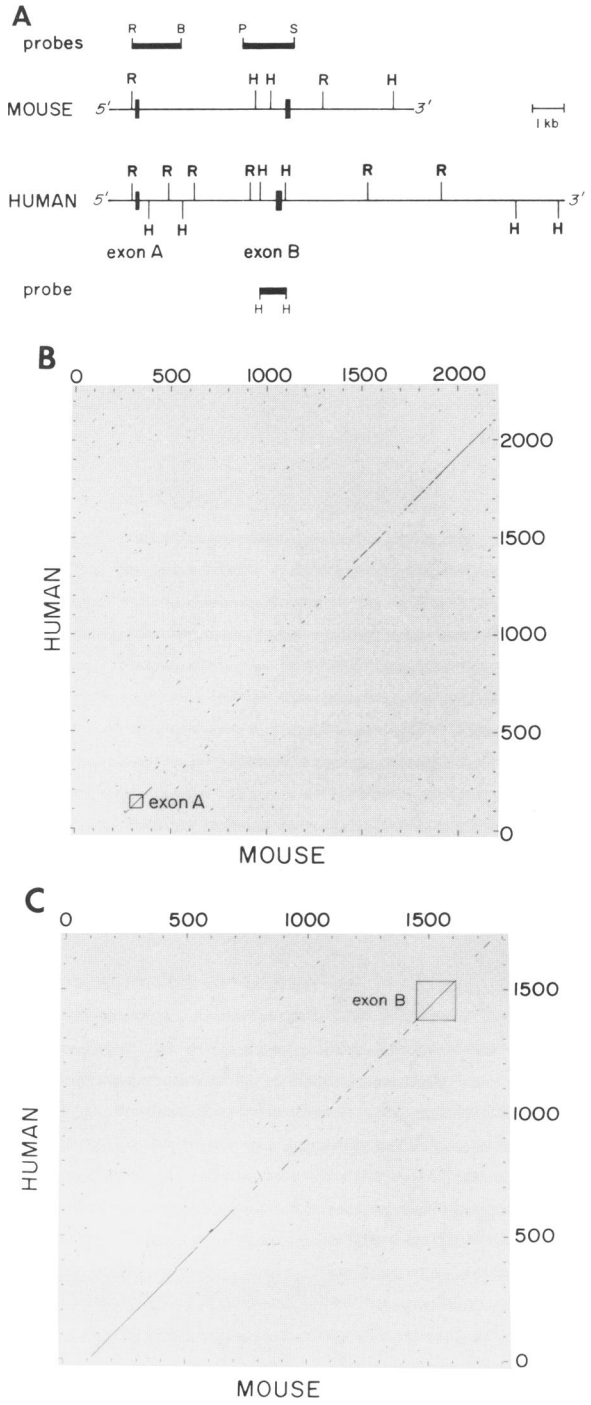

Figure 1 *A*, Restriction map of related mouse and human genomic DNA corresponding to mouse limb deformity locus showing *Eco*I (R) and *Hin*dIII (H) sites. Also shown are mouse (*upper*) and human (*lower*) genomic fragments used as probes (*Bgl*II [B], *Pvu*II [P], and *Sau*3A [S]). The mouse map was derived from a lambda phage clone containing a 15-kb *Bam*HI-*Bam*HI fragment (Woychik et al. 1985). The human map was derived from a lambda phage clone λ3-1 in vector EMBL3. The location of the two conserved exons denoted A and B are shown. *B*, Dot-matrix comparison of nucleotide sequence determined from related mouse and human regions, over 2-kb region, surrounding exon A in panel *A*. The comparison was run at a stringency of 14 of 21 bp. Conserved exon A, consisting of 52 bp, is shown, *C*, Dot-matrix comparison of nucleotide sequence determined from related mouse and human genomic DNA surrounding exon B over 2-kb region. The comparison was run at a stringency of 14 of 21 bp. Conserved exon B, consisting of 150 bp, is shown.

curs at a time associated with appearance of the mutant phenotype; and, finally, disrupted transcripts are observed in three of the five existing *ld* mutants (Maas et al. 1990; T. F. Vogt, personal communication).

The similarity between human and mouse sequences creates the opportunity to identify molecular probes to test for linkage of the homologous human locus to hereditable human limb and kidney deformities such as syndactyly and renal aplasia. Despite the possibility that identical mutations in homologous genes on human and murine genetic backgrounds might yield different phenotypes, it has been proposed that there may be homologous sets of mouse and human malformation syndromes (Gruenberg 1971; Winter 1988), along with a set of criteria for identifying homologous genes between different species (Lally and McKusick 1985).

We now describe sequence and restriction-mapping data for a human genomic clone, which contains two major human-mouse homology regions, each containing sequences which are represented as exons in mRNA. This human gene, to which we have assigned the locus symbol "LD, is related to the mouse formin gene by extraordinary sequence similarity both in these exons and in adjacent flanking regions and is localized to the long arm of chromosome 15. In addition we have identified two independent RFLPs which may prove useful in testing the linkage of human disorders potentially related to mutations in the LD gene.

Material and Methods

Genomic Cloning

A human genomic library prepared in the vector EMBL3 was a gift from Ed Fritsch. Approximately 800,000 plaques were screened with a 1.5-kb *Pvu*II-*Sau*3A mouse DNA fragment described elsewhere (Woychik et al. 1985) and shown in figure 1*A*. Three positive clones were identified, carried to plaque purification, grown in 1-liter cultures, and phage purified by discontinuous cesium chloride gradient for DNA preparation (Sambrook et al. 1989).

Restriction Mapping and DNA Sequence Determinations

Subcloning and DNA sequence determinations were carried out by standard methods using Sanger dideoxy sequencing in M13 (Sanger et al. 1977) and by sequencing of denatured double-stranded plasmid templates (Chen and Seeberg 1985) by using T7 polymerase (Sequenase; U.S. Biochemicals).

RNA Isolation and RNAse Protection Assays

Total RNA was isolated from human fetal tissues obtained in compliance with guidelines established by the institutional review board at Brigham and Women's Hospital, from 20-wk abortuses. Human tumor tissue was obtained from freshly obtained surgical or autopsy specimens. RNA was isolated from guanidinium isothiocyanate–cesium chloride gradients and was quantitated by absorption at 260 nm (Chirgwin et al. 1979). One RNAse protection probe employed was a 570-nucleotide (nt) fragment prepared by SP6 transcription of an *Xho*I-linearized pGEM3 plasmid containing the 850-bp *Hin*dIII-*Hin*dIII human genomic fragment containing exon B, as shown in figure 1*A*. A second probe corresponding to exon A was prepared by subcloning a 510-bp *Hin*dIII-*Eco*RI fragment into pGEM3, linearization with *Eco*RI, and in vitro transcription with SP6 polymerase. In both cases, the probes were labeled using [α-^{32}P]-UTP, 800 Ci/mmol. RNAse protection was performed according to a method described elsewhere (Krieg and Melton 1987), using 50–72 μg of total human fetal RNA, followed by analysis on a 6% denaturing polyacrylamide gel and autoradiography for 12–36 h.

Somatic Cell Hybrid Mapping

DNA was obtained from human-rodent somatic cell hybrids (Shows et al. 1978, 1982, 1984; Shows 1983) and was digested with *Pvu*II. This enzyme was chosen because, in the mouse, *Eco*RI gave a cross-hybridizing band of a size very similar to the 6.6-kb band observed in human genomic DNA. The 0.85-kb human *Hin*dIII-*Hin*dIII fragment (see fig. 1*A*), devoid of repetitive sequence, was nick-translated with [α-^{32}P]-dCTP, 3,000 Ci/mmol and was used as a probe in this analysis. Concordance and discordance were tabulated in standard fashion.

Chromosomal In Situ Hybridization

The chromosomal location of the human homologue of the mouse *ld* gene was determined using a [^{3}H]-dCTP, -dATP, and -dTTP random hexamer-labeled probe prepared from the same 0.85-kb *Hin*dIII-*Hin*dIII fragment used in the somatic cell hybrid-mapping experiments. Metaphase chromosome spreads were prepared from BrdUrd-synchronized lymphocyte cultures. In situ hybridization was carried out according to methods described elsewhere (Zabel et al. 1983; Nakai et al. 1986). Grains were counted from a random selection of 100-well banded metaphase spreads with no more than five background grains per spread.

RFLP Analyses

DNA isolated from six different unrelated individuals was digested with restriction enzymes, electrophoresed, transferred to nitrocellulose, and probed with the 0.85-kb *Hin*dIII-*Hin*dIII fragment. The enzymes tested are given in Results. Additional DNA samples were tested and analyzed as described in Results.

Results

Isolation and Characterization of Human Genomic Clone

A 1.7-kb *Pvu*II-*Sau*3A mouse genomic fragment derived from the region flanking the *ld*^{Hd} transgene insertion site (see fig. 1*A;* also see Woychik et al. 1985) was observed to hybridize to a single human *Eco*RI genomic DNA fragment under conditions of moderate stringency (55°C, 0.2 × SSC, 0.1% SDS). This mouse probe was subsequently used to screen a human genomic lambda phage library, and three clones were plaque purified and restriction mapped. Two of these, which were identical, gave the restriction map shown in figure 1*A*. A third clone, containing an apparent rearrangement, was not characterized further.

A second human genomic region (denoted "exon A" in fig. 1*A*) was identified by Southern blotting analyses at moderate stringency by using a 1.7-kb mouse *Eco*RI-*Bgl*II fragment to probe human *Eco*RI-digested genomic DNA. This blot revealed two small cross-hybridizing *Eco*RI fragments of 1.1 and 0.8 kb. This region was also found to reside on the same phage clone as that identified with the 1.7-kb mouse *Pvu*II-*Sau*3A fragment. The nucleotide sequence of the mouse *Eco*RI-*Bgl*II fragment, along with a small amount of sequence on both sides of these restriction sites, was determined and compared with 2.2-kb of cross-hybridizing human sequence which was analyzed as a series of *Eco*RI-*Hin*dIII M13 and pGEM clones. This sequence comparison, shown in dot-matrix form in figure 1*B*, reveals these two main regions of homology. One of these regions, denoted "exon A" in figure 1*B*, showed a 52-bp ORF bounded

by canonical splice-acceptor and splice-donor sequences (Mount 1982) which is conserved at 51 of 52 nucleotides and at all deduced amino acid positions in sequences from both species. (These sequences are available from GenBank, under accession numbers listed in Acknowledgments.)

The region noted to cross-hybridize initially, defined by the mouse 1.7-kb *Pvu*II-*Sav*3A fragment which hybridized with 6-kb *Eco*RI and 0.85-kb *Hin*dIII human fragments, was also analyzed. The nucleotide sequence of approximately 1.8 kb of the human genomic clone was determined in this region and was compared with the mouse sequence, and three main regions of extensive homology were noted, as shown in dot-matrix form in figure 1*C*. One of these regions, denoted "exon B" in figure 1*A* and *C*, demonstrated a conserved 150-bp ORF bounded by splice-acceptor and splice-donor sequences. Both putative exons A and B predict a transcription unit oriented in the same direction in the genome. Strand-specific RNA probes to these mouse sequences, prepared using SP6 polymerase, were found to detect a large differentially processed family of transcripts in various murine tissues (Woychik et al. 1990*b*). Further analysis has revealed that the sequences denoted "exon A" and "exon B" are in fact adjacent exons in this transcription unit, which encodes a group of deduced formin proteins. Accordingly, we undertook to determine whether an analogous pattern of expression could be identified for the similar human sequences.

Expression of Human Exonic Sequences

RNA was obtained from a variety of human fetal tissues, and 50 μg from each tissue was analyzed by an RNAse protection assay using a strand-specific probe encompassing putative exon B. The expected size of the protected fragment should be 150 bp, as predicted by comparison of the mouse and human sequences. Of note, expression of transcripts containing the 150-bp exon is seen in a wide variety of human fetal tissues, as previously observed for the mouse gene in adult and embryonic mouse tissues. Particularly abundant expression was observed in human fetal kidney and lung (fig. 2*A*). It is interesting that, when 50 μg of RNA from several human tumor samples was analyzed (fig. 2*A*), abundant expression was noted in a

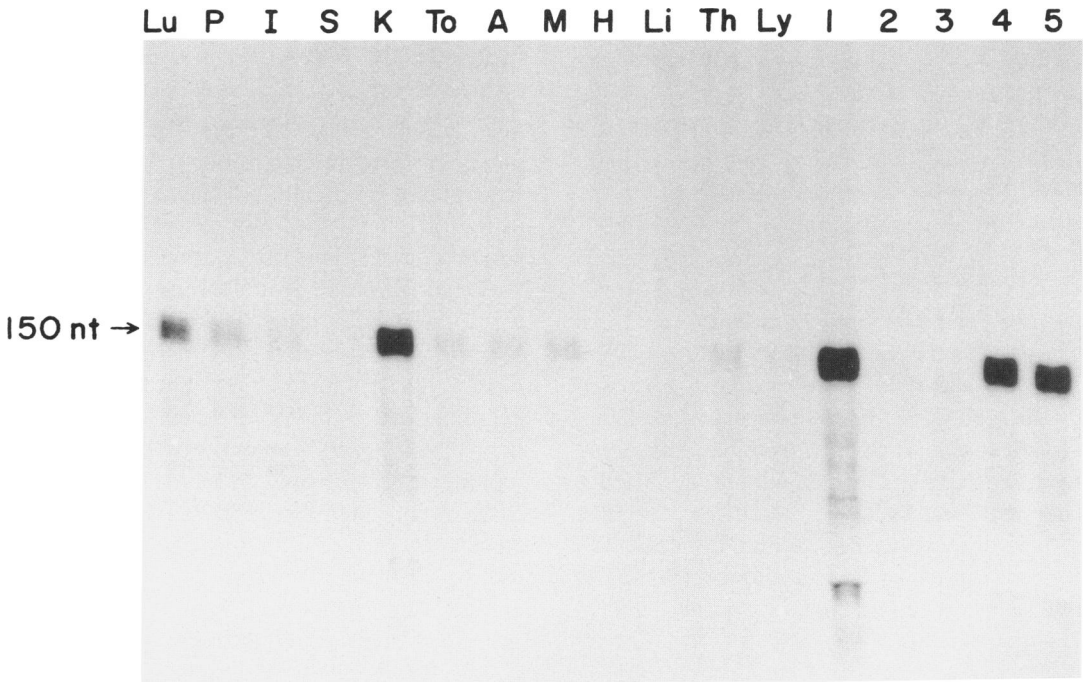

Figure 2 RNAse protection experiment employing human fetal RNA and SP6 transcribed probe derived from human exon B. The predicted 150-nt protected fragment is observed. Samples (50-μg) of a variety of tissue RNAs (lettered lanes) and five different tumor-sample RNAs (lanes 1–5) were analyzed. A tRNA control (not shown) was blank. Lu = lung; P = placenta; I = small intestine; S = spleen; K = kidney; To = tongue; A = adrenal; M = muscle; H = heart; Li = Liver; Th = Thymus; Ly = lymph node; 1 = renal cell carcinoma; 2 = hepatoma; 3 = Burkitt cell lymphoma; 4 = small-cell carcinoma of lung; 5 = lung carcinoma.

Table 1

Segregation of DNA Probe for Human *Limb Deformity* with Human Chromosomes in *Pvu*II-digested Human-Mouse Cell Hybrid DNA

Hybrid Type	No. Observed, by Chromosome																					
	1	2	3	4	5	6	7	8	9	10	11	12	13	14	15	16	17	18	19	20	21	22	X
Concordant:																							
+/+	7	11	13	11	11	9	10	12	5	14	8	14	10	13	18	6	15	13	8	11	15	9	11
−/−	14	12	10	8	10	13	8	12	14	8	9	11	10	9	16	16	4	12	12	6	5	10	4
Discordant:																							
+/−	9	7	6	8	8	10	8	7	12	5	9	5	9	6	0	13	4	6	11	8	4	10	7
−/+	1	5	6	9	7	4	8	5	3	8	8	6	7	8	0	1	13	5	5	11	12	6	9
Total no. (%) discordant	10 (32)	12 (34)	12 (34)	17 (47)	15 (42)	14 (39)	16 (47)	12 (33)	15 (44)	13 (37)	17 (50)	11 (31)	16 (44)	14 (39)	0 (0)	14 (39)	17 (47)	11 (31)	16 (44)	19 (53)	16 (44)	16 (46)	16 (52)

NOTE.—Table is compiled from 36 cell hybrids involving 14 unrelated human cell lines and four mouse cell lines. The hybrids were characterized by karyotypic analysis and by mapped enzyme markers. The DNA probe for the human limb deformity was hybridized to Southern blots containing *Pvu*II-digested DNA from the human-mouse hybrids. Scoring for the probe was determined by the presence (+) or absence (−) of a human band in the hybrids on the blots. The scoring was compared with the presence or absence of human chromosomes in each hybrid. A 0% discordancy indicates a matched segregation of the probe with a chromosome and is the basis for chromosome assignment from the given hybrid panel. The DNA probe for human limb deformity mapped to human chromosome 15 by somatic cell hybrids. The hybrids DUA-1A and DUA-1CSAZB with the der(X) and der(15) tranlocations—Xter→Xp11::15q11→15qter and 15pter→15q11::Xp11→Xpter, respectively—further localize this gene to the q11→qter region of human chromosome 15 (see fig. 3).

renal cell carcinoma and in small-cell and non–small cell carcinomas of the lung but not in a hepatoma or Burkitt lymphoma. These results are consistent with the observation that both kidney and lung are major sites of expression among normal tissues.

The expression data noted above were confirmed using the smaller of the two putative human exons (i.e., exon A, a 52-bp sequence), with human fetal kidney being the major site of expression. These results indicate that the human sequences A and B are in fact exons of an expressed human gene related to the mouse formin gene. Since, on the basis of high- and low-stringency Southern analyses (data not shown), these sequences appear to be single or low copy number in the human genome, we conclude that the mouse and human sequences are likely to be homologous.

Human-Rodent Somatic Cell Hybrid Mapping

To determine the chromosomal location of the human locus, the 0.85-kb human *Hin*dIII-*Hin*dIII fragment (see fig. 1*A*) was used as a probe to detect human DNA fragments on a mouse-human somatic cell panel (table 1). This analysis shows concordance only with human chromosome 15. Of further note, two deletion derivatives of human chromosome 15 which contain only the short or long arm were included in the analysis. The results obtained with these lines (fig. 3) further localize the human locus to 15q11→qter and exclude 15pter→q11.

Chromosomal In Situ Hybridization

To further define the assignment of the cloned human sequences, in situ hybridization of the 0.85-kb human *Hin*dIII-*Hin*dIII fragment to human metaphase chromosomes was performed. This analysis showed that the human fragment hybridized primarily to the long arm of human chromosome 15 and specifically to the q13→q14 region. Of 100 metaphases analyzed and 154 grains counted, 20 grains (13%) localized to the 15q13→q14 region, with 14 grains over q14 and six over q13 (fig. 4*B*). Thus, the human homologue of the mouse formin gene resides at 15q13→q14.

RFLP Analysis

To determine whether the isolated human probes identified any RFLPs in the human genome, the 0.85-kb *Hin*dIII-*Hin*dIII probe was tested against human genomic DNAs isolated from six unrelated individuals. RFLPs were identified with the enzymes *Acc*I and *Hin*cII (fig. 5). The following enzymes failed to yield polymorphisms: *Ava*II, *Bam*HI, *Ban*I, *Bgl*II, *Dde*I,

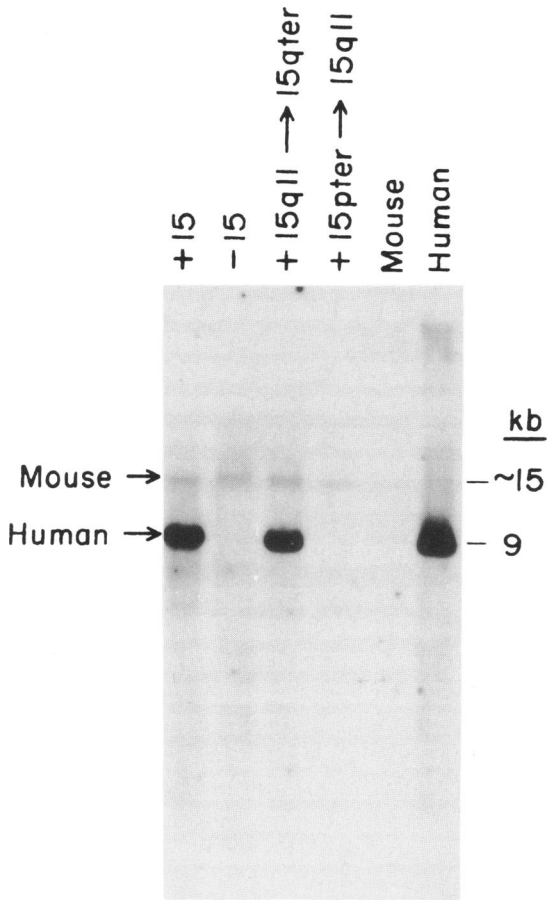

Figure 3 Human-rodent somatic cell mapping panel, with deletion derivatives of human chromosome 15 and 0.85-kb *Hin*dIII-*Hin*dIII fragment shown in fig. 1*A* used as probe against *Pvu*II-digested DNAs. The hybridizing *Pvu*II fragment at about 15 kb, present in all samples except for human DNA, corresponds to the cross-hybridizing mouse sequence; the hybridizing *Pvu*II fragment at 9 kb is the human sequence.

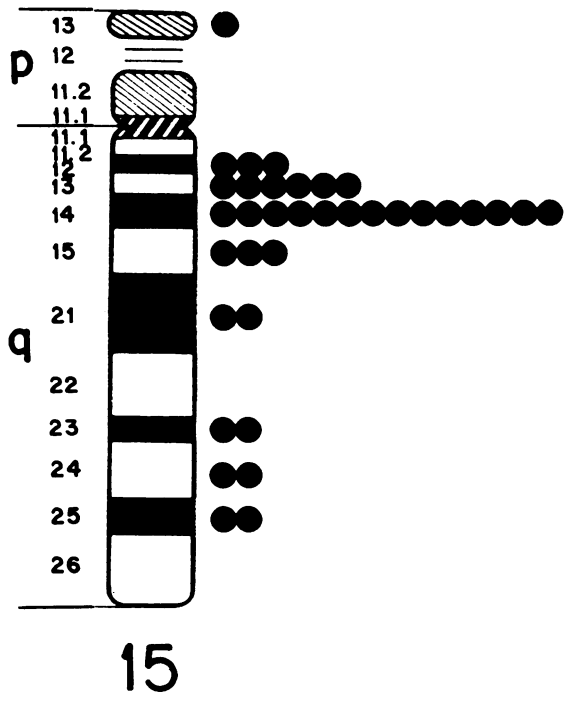

Figure 4 In situ hybridization results showing distribution of grains hybridizing to human chromosome 15 and localization to 15q13→q14.

*Eco*RI, *Eco*RV, *Hin*dIII, *Hin*fI, *Msp*I, *Rsa*I, *Pst*I, *Pvu*II, *Ssp*I, *Taq*I, and *Xba*I. Two allele systems were identified for each of the polymorphisms, with 11-kb (allele A) and 6.5-kb (allele B) *Acc*I fragments and 9.5-kb (allele C) and 8.0-kb (allele D) *Hin*cII fragments. To define further the frequency of these alleles in the population, 21 additional DNAs were digested with *Acc*I and 24 additional DNAs were digested with *Hin*cII. Allele frequencies from this analysis are summarized in table 2. The observed heterozygosities (determined as number of heterozygotes per total number of observations) are .52 for the *Acc*I polymorphism and .60 for the *Hin*cII polymorphism. Calculated from the product of the individual allele frequencies, the expected haplotype frequencies are as follows: AC, .44; AD, .26; BC, .19; and BD, .11. This compares with the observed frequencies—AC, .63; AD, .23; BC, .13; and BD, .00 ([χ^2 = 6.56] when individuals of ABCD genotype who are haplotype uninformative are not considered). Since recalculation of the expected haplotype frequencies after exclusion of the doubly heterozygous ABCD individuals yields much closer agreement with the observed haplotype frequencies, and because some of the individuals used in this analysis were related to one another, no conclusions about linkage equilibrium or disequilibrium are possible.

The Mendelian segregation of these independent polymorphisms recognized with the same molecular probe was demonstrated in an additional experiment, using DNAs isolated from two families. These results, shown for one family's DNA digested with each enzyme (fig. 5), confirm the codominant inheritance of both *Acc*I and both *Hin*cII alleles.

Discussion

One reason to report on the mapping of the human

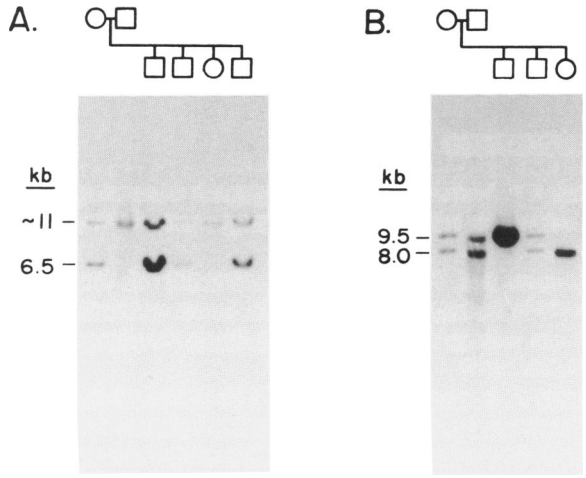

Figure 5 RFLP analysis showing Southern blot of family pedigree of human DNAs digested with enzymes *Acc*I (A) and *Hin*cII (B), probed with 0.85-kb *Hin*dIII-*Hin*dIII fragment described in text. Enzymes tested and not found to yield polymorphisms are described in Results. The approximate sizes of the hybridizing fragments are shown in kilobases (kb).

Table 2

Allele Frequencies for Two-Allele RFLPs at Human LD Locus

Frequency for			
*Acc*II ($n = 27$)		*Hin*cII ($n = 30$)	
A	B	C	D
.70	.30	.63	.37

Note.—A allele—11.0-kb *Acc*I fragment; B allele—6.5-kb *Acc*I fragment; C allele—9.5-kb *Hin*cII fragment; D allele—8.0-kb *Hin*cII fragment. Heterozygosities: *Acc* II, .52; *Hin*cII, .60. The indicated number of genomic DNA samples were digested with the restriction enzyme indicated and were analyzed by Southern blotting. The probe used was the 0.85-kb *Hin*dIII-*Hin*dIII human genomic fragment described in Material and Methods and indicated in fig. 1*A*. The frequency of the indicated alleles was counted and tabulated; no other patterns of hybridizing fragments were observed.

LD locus at the present time is that the *ld* locus, at least in the mouse, is exceedingly complex, making a comprehensive characterization of the gene difficult. The murine gene residing at this locus is estimated to span more than 100 kb, with evidence for numerous modes of differential processing, resulting in a large family of different transcripts (Woychik et al. 1990*b*; L. Jackson-Grusby, personal communication). On the basis of the similarity between mouse and human exons A and B at the sequence level and at the level of RNase protection, it seems likely that the human locus will be similarly complex. We wished therefore to map and characterize our initial human clone such that it might be available for studying linkage to any potentially relevant human genetic disorders. From this striking exon-structure similarity between the mouse and human genes, albeit limited to two exons, we conclude that we have correctly identified the homologous human locus. In addition, Southern-blotting results with the probes described here indicate that these are single-copy sequences in the human genome. Thus, the possibility that we have identified a related but nonorthologous gene in the human genome seems unlikely.

The mapping of the human LD locus to chromosome 15q13→q14 is noteworthy in that it, as well as β_2-microglobulin, sorbitol dehydrogenase, and cardiac α-actin, are syntenic in the mouse and human genomes (Cox and Donlon 1989). It will be of interest to determine whether gene order and linkage distances as determined in the mouse will apply to corresponding human genes. On the other hand, several other mouse loci linked to *ld* on mouse chromosome 2—e.g., catalase—have been mapped to human chromosome 11. These results are not inconsistent, because the order of the loci in the mouse has been determined by recombinant inbred crosses (Glaser et al. 1990) and because the mouse *ld* locus maps between β_2-microglobulin and catalase. It thus appears that, during mammalian evolution, genes present on mouse chromosome 2 have been split between human chromosomes 11 and 15, with the presumptive division point occurring between the murine catalase and *ld* loci. Conversely, human chromosome 15 also contains genes whose corresponding mouse loci are on chromosomes 7 and 9.

Although, given the involvement of the kidney in the *ld* phenotype, the finding that the human fetal kidney is a major site of expression of the human LD locus is an appealing one, this may not necessarily explain the renal aplasia phenotype. Previously, Zeller et al. (1989) observed a fivefold regional enhancement of expression of the murine *ld* gene in limb bud ectoderm (AER) relative to mesoderm and suggested a model whereby, in the mutant, larger decremental expression in ectoderm relative to mesoderm correlated with a morphometrically demonstrable reduction in amount of AER. The observation of abundant expression in the the 20-wk-gestation human fetal kidney,

however, cannot be interpreted in analogous fashion. First, human renal development at the 20-wk stage (second trimester) is nearly complete in all important respects, especially morphologically. In the *ld/ld* mouse and in the chick embryo, renal agenesis can be linked to a deficiency in the proper outgrowth of the ureteric bud and not to a deficiency in metanephric mesenchyme which comprises the renal anlage. Moreover, the morphologic abnormality in the ureteric bud can be observed at day 11 of mouse embryogenesis, a stage before subsequent tubular differentiation has begun (R. L. Maas, unpublished data). Thus it would be of interest to investigate expression of LD transcripts in the ureteric bud at earlier stages (i.e., prior to 30 d) of human embryonic development.

The identification of two RFLPs by a probe associated with the putative human LD locus should permit the linkage testing of several human limb and/or renal dysmorphoses. Of note, there are several unmapped, presumably recessive human syndromes which share deformities of the appendicular skeleton and kidneys, including variants of Cenani-Lenz syndactyly (Pfeiffer and Meisel-Stosiek 1982), polysyndactyly–double pyeloureteral system syndrome (Conde et al. 1978), and cryptopthalmos-syndactyly (Lurie and Cherstvoy 1984). In addition, unilateral renal agenesis is estimated to be one of the most common congenital malformations, occurring in approximately 1/1,000 individuals, and familial inheritance of this condition has been reported (Emanuel et al. 1974). On the other hand, none of these human syndromes conforms closely to the phenotype observed in the mouse *ld/ld* mutants, and, moreover, it is likely that unilateral renal agenesis has several different etiologies. In particular, any factor, either genetic or environmental, which alters the growth of the ureteric bud has the potential to result in a failure of renal growth. Nonetheless, it will be important to complete the characterization of the human locus and to establish its role, if any, in human embryonic development.

Acknowledgments

Portions of this work were supported in part by a grant from E. I. Dupont de Nemours Co., Inc. The authors are grateful to Dr. Jonathan Haines for assistance in the calculation of the haplotype frequencies. Four blocks of DNA sequence data relevant to the present paper have been deposited in GenBank (Los Alamos). These correspond to genomic DNA surrounding mouse (accession no. M38686) and human (accession no. M38684) exon A and mouse (accession no. M38687) and human (accession no. M38685) exon B, as shown in figure 1*A*.

References

Chen EY, Seeberg PH (1985) Supercoil sequencing: a fast and simple method for sequencing plasmid DNA. DNA 4:165–170

Chirgwin JM, Przybala AE, MacDonald RJ, Rutter WJ (1979) Isolation of biologically active ribonucleic acid from sources enriched in ribonuclease. Biochemistry 18: 5294–5299

Conde F, Gomez S, Massa C (1978) Polysyndactyly with double pyeloureteral system. An Esp Pediatr 11:237–240

Cox DW, Donlon TA (1989) Report of the Committee on the Genetic Constitution of Chromosomes 14 and 15. Human Gene Mapping 10. Cytogenet Cell Genet 51:280–298

Emanuel B, Nachman R, Aronson N, Weiss H (1974) Congenital solitary kidney: a review of 74 cases. J Urol 111: 394–397

Glaser T, Lane J, Housman D (1990) Dickie's small eye mutation (*Sey*^{Dey}): a mouse model of the aniridia–Wilms tumor deletion syndrome. Science 250:823–827

Green MC (1981) Catalog of mutant genes and polymorphic loci. In: Genetic variants and strains of the laboratory mouse. Gustav Fischer, New York, p 137

Gruenberg H (1971) Brachypodism in the mouse. Birth Defects 13:221–230

Kleinebrecht J, Selow J, Winkler W (1982) The mouse mutant limb-deformity (ld). Anat Anz 152:313–324

Krieg PA, Melton DA (1987) In vitro RNA synthesis with SP6 RNA polymerase. Methods Enzymol 155:397–415

Lally PA, McKusick VA (1985) Report of the Committee on Comparative Mapping. Human Gene Mapping 8. Cytogenet Cell Genet 40:536–566

Lurie IW, Cherstvoy ED (1984) Renal agenesis as a diagnostic feature of the cryptopthalmos-syndactyly syndrome. Clin Genet 25:528–532

Maas RL, Zeller R, Woychik RP, Vogt TF, Leder P (1990) Formin-encoding transcripts are disrupted in two mutant limb deformity alleles. Nature 346:853–855

Messing A, Behringer RR, Slepak JR, Lemke G, Palmiter RN, Brinster RL (1990) Insertional mutation at the LD locus (again!) in a line of transgenic mice. Mouse Newslett 87:107

Mount SM (1982) A catalogue of splice junction sequences. Nucleic Acids Res 10:459–472

Nakai H, Byers MG, Shows TB, Taggart RT (1986) Assignment of the pepsinogen gene complex (PGA) to human chromosome region 11q13 by in situ hybridization. Cytogenet Cell Genet 43:215–217

Pfeiffer RA, Meisel-Stosiek M (1982) Present nosology of the Cenani-Lenz type of syndactyly. Clin Genet 21:74–79

Sambrook J, Fritsch EF, Maniatis T (1989) Bacteriophage λ vectors. In: Molecular cloning: a laboratory manual. Cold Spring Harbor Laboratory, Cold Spring Harbor, NY, pp 2.69–2.81

Sanger F, Brownlee GG, Coulson AR (1977) DNA sequencing with chain terminating inhibitors. Proc Natl Acad Sci USA 74:5463–5467

Shows T, Eddy R, Haley L, Byers M, Henry M, Fujita T, Matsui H, et al (1984) Interleukin 2 (IL2) is assigned to human chromosome 4. Somatic Cell Mol Genet 10:315–318

Shows TB (1983) Human genome organization of enzyme loci and metabolic diseases. In: Rattazzi MC, Scandalios JG, Whitt GS (eds) Isozymes: current topics in biological and medical research. Vol. 10. Alan R Liss, New York, pp 323–339

Shows TB, Brown JA, Haley LL, Byers MG, Eddy RL, Cooper ES, Goggin AP (1978) Assignment of the β-glucronidase structural gene to the pter→q22 region of chromosome 7 in man. Cytogenet Cell Genet 21:99–104

Shows TB, Sakaguchi AY, Naylor SL (1982) Mapping the human genome, cloned genes, DNA polymorphism, and inherited disease. In: Harris H, Hirschorn K (eds) Advances in human genetics. Vol 12. Plenum, New York and London, pp 341–452

Winter RM (1988) Malformation syndromes: a review of mouse/human homology. J Med Genet 25:480–487

Woychik RP, Generoso WM, Russell LB, Cain KT, Cacheiro NLA, Bultman SJ, Selby PB, et al (1990*a*) Molecular and genetic characterization of a radiation induced structural rearrangement in mouse chromosome 2 causing new mutations at the limb deformity and agouti loci. Proc Natl Acad Sci USA 87:2588–2592

Woychik RP, Maas RL, Zeller R, Vogt TF, Leder P (1990*b*) The formins: a novel class of proteins deduced from the alternative transcripts of the limb-deformity gene. Nature 346:850–853

Woychik RP, Stewart TA, Davis LG, D'Eustachio P, Leder P (1985) An inherited limb deformity created by insertional mutagenesis in a transgenic mouse. Nature 318:36–40

Zabel BU, Naylor SL, Sakaguchi AY, Bell GI, Shows TB (1983) High resolution chromosomal localization of human genes for amylase, proopiomelanocortin, somatostatin, and a DNA fragment (D3S1) by in situ hybridization. Proc Natl Acad USA 80:6033–6036

Zeller R, Jackson-Grusby L, Leder P (1989) The limb deformity gene is required for apical ectodermal ridge differentiation and anteroposterior limb pattern formation. Genes Dev 3:1481–1492